Modal Interaction in a Levitation Force MEMS Based Resonator

Conference Paper · November 2021

DOI: 10.1115/IMECE2021-72755

4 authors:

Mohammadreza Zamanzadeh
Urmia University
12 PUBLICATIONS **128** CITATIONS
SEE PROFILE

Hil G E Meijer
University of Twente
106 PUBLICATIONS **1,293** CITATIONS
SEE PROFILE

Ilgar Jafarsadeghi-Pournaki
Urmia University
14 PUBLICATIONS **165** CITATIONS
SEE PROFILE

Hassen Ouakad
Sultan Qaboos University
127 PUBLICATIONS **1,758** CITATIONS
SEE PROFILE

Proceedings of the ASME 2021
International Mechanical Engineering Congress and Exposition
IMECE2021
November 1-5, 2021, Virtual, Online

IMECE2021-72755

MODAL INTERACTION IN A LEVITATION FORCE MEMS BASED RESONATOR

Mohammadreza Zamanzadeh[1], H. G. E. Meijer[2,*], Ilgar Jafarsadeghi-Pournaki[1], H. M. Ouakad[3,*]

[1]Department of Mechanical Engineering, Urmia University, Urmia, Iran
[2]Department of Applied Mathematics, University of Twente, Enschede, Netherlands
[3]Mechanical and Industrial, Engineering Department, College of Engineering, Sultan Qaboos University, Muscat, Oman

ABSTRACT

This work aims to examine the possibility of internal resonances (modal interactions) among the vibration modes of a levitation force Micro-electro-mechanical Systems (MEMS) based resonator. The actuating levitation force is generated through a special arrangement consisting of two stationary side electrodes (both electrically charged) and a middle grounded unit consisting of the stationary electrode located beneath a moving electrode (micro-beam). Both "cantilever" (CL) and "clamped-clamped" (CC) microbeams are analysed as the moving element of this especial design in which the applied voltage pushes away the micro beam from the underneath substrate. All possible commensurable relations between the frequencies are inspected. We use the numerical bifurcation toolbox MatCont to capture the computed frequency response branches and examine their stability. A period-doubling bifurcation for the possible onset of chaotic attractors is inspected as well. A preliminary eigenvalue problem analysis suggests the internal resonance may exist in both (CC and CL) cases. However, an extended dynamical analysis shows that just a 3-to-1 modal interaction (between the first and third modes) in the CC arrangement is possible. The effects of dominant force-related terms are plotted through associated plots. These diagrams demonstrated that this design exhibits a rich internal resonance behavior that can be controlled with different geometrical and actuating parameters. Overall, this effort provides a systematic methodology and simple guidelines for in-depth exploration of internal resonances in levitation force-based microbeams. The outcomes of this work could also assist in the development of MEMS sensors based on the internal resonance phenomenon.

1. INTRODUCTION

Levitation force Micro-electro-mechanical Systems (MEMS) configuration is a kind of device in which the applied voltage pushes away the moving part from the stationary electrode underneath. The upward electric force in this pull-in free structure is generated via a special arrangement by adding two lateral substrates and applying the same voltage to these side units while the middle unit is grounded [1, 2]. This innovative design owns numerous advantages as compared to the classical parallel-plates counterpart, such as the possibility of bouncing back [3] rather than experiencing a pull-in instability (micro-stiction, short circuit) [4–7], the double-side tunability [8] against mere mono-side tunability with increasing frequency shift, pairability with parallel plate [9] for releasing the latched micro-beam, a higher resolution and broader range for pressure/mass detection [10] and better durability with more reliable performance for switch application [11]. In almost all of the literature concerning levitation force MEMS layout, one mode assumption has been used to simplify the derivation of the governing equation of motion. This simplification comes at the expense of missing some system characteristics limiting the proper prediction of the dynamical behavior.

Internal resonance emerges from the energy transfer between the vibration modes, which have promising applications for functional improvement in MEMS [12, 13]. The prerequisites for such a modal interaction in MEMS with parallel plate structure have been defined by Younis et al. [14] based on classical theory. Adopting modified coupled stress theory, Ghayesh et al. [15] studied the modal interaction considering the effect of size, the length-scale parameter, and curvature nonlinearities on the overall dynamical response. Recently, Kumar et al. [16] characterized all possible internal resonances within a clamped-clamped micro resonator and how to tolerate the internal resonance by adjusting the external force, and geometrical and material properties. In almost all the investigations on internal resonance, the standard indirect and time-consuming semi-analytical techniques (such as perturbation analysis) require re-writing the governing equation of motion based on the magnitude of the standing terms. This approach is followed by balancing the terms and leading to conditionally valid and invalid responses based on the prejudgment

*Corresponding author: houakad@squ.edu.om

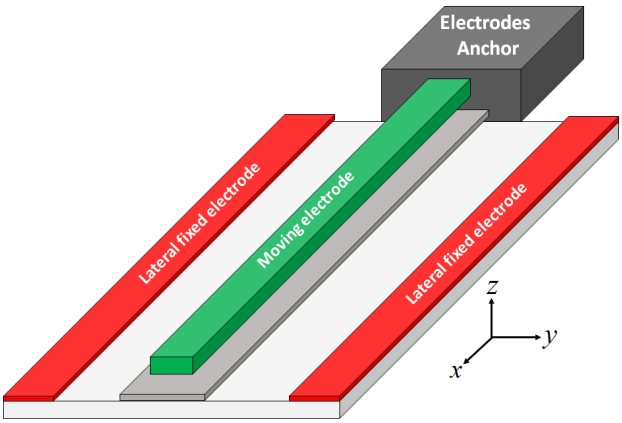

(a) cantilever (CL)

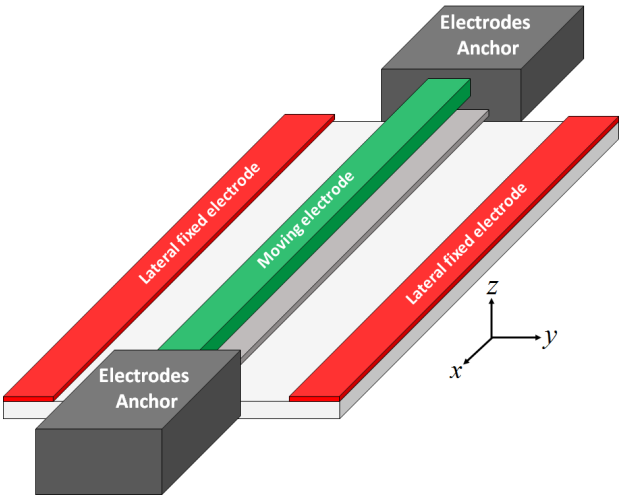

(b) clamped-clamped (CC)

FIGURE 1: 3D view of the levitation force MEMS actuator in two cases.

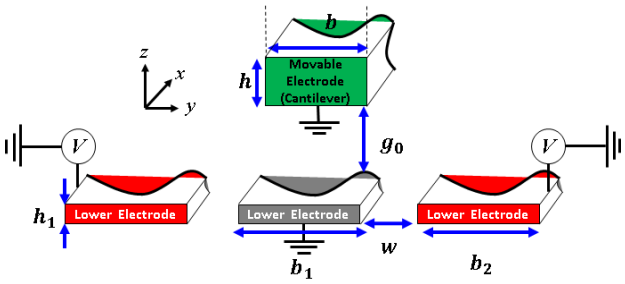

(a) 2D schematic front view of the arrangement displaying the electrical and geometrical characteristics in which the side electrodes are charged and the middle ones are grounded.

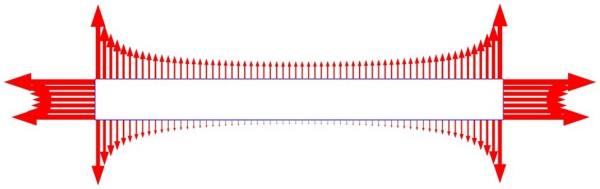

(b) 2D finite element simulation for electric force distribution around the boundaries of moving electrode. The upward and downward arrows represents the repulsive and attractive force respectively.

FIGURE 2: Schematic view for the geometrical and electrical characteristics of the levitation force MEMS segments.

of the magnitude for the dominant terms.

Another MEMS structure exhibiting strong energy exchange is an arch-shaped MEMS device with initial rising or divulging in the moving segment. Ouakad et al. [17] conducted an exhaustive investigation of internal resonance with the method of multiple scales. They proved the effect of the initial rise and mid-plane stretching on triggering the modal energy exchange, which might be intrinsic at first glance. Other phenomena like jumping and bifurcations arising from the modal interaction of three to one internal resonance were explored by Wang et al. [18]. Typical analyses involved Poincaré sections, and the Fast Fourier Transformation (FFT) further indicated the necessity of taking higher modes into account for a comprehensive study of the MEMS structure and detection of modal interaction. From the literature review, we realized that higher modes for levitation force MEMS structure and modal interactions to-date ignored to-date, although their effect has been studied extensively for other kinds of MEMS systems. Here, we study their effect employing a more straightforward approach using the numerical bifurcation toolbox MatCont. As the modes are weakly stable, this approach is much faster than the simulation approach, and we capture the complex response branches of the system accurately. The continuation approach allows us to determine stability, detect bifurcations, and perform branch switching for our exhaustive survey.

In section 2, we describe the geometry of our MEMS device and the governing equation of motion. Section 3 provides details of our analysis using MatCont followed by the results in section 4. The highlights are summarized and discussed in section 5.

2. MODEL DESCRIPTION AND SYSTEM FORMULATION

The proposed repulsive force actuator's design consists of a suspended clamped-clamped (CC) or/cantilever (CL) moving electrode, a fixed middle electrode placed directly underneath the moving one, and two side electrodes, as shown in Fig. 1. The levitation force is generated by applying the same voltage to the side electrodes while the middle unit is grounded as displayed in Fig. 2a or by grounding the side electrodes and applying the same voltage to the subcomponents of the middle unit. Subsequently, the finite element (FE) analysis of the distributed net force on the borders of the moving part (see Fig. 2b) implies the resulting upward force that lifts the moving electrode away from the substrate.

TABLE 1: Geometrical and Material Properties of the Repulsive Force Actuator

Parameter	Symbol	value
Middle beam length (Clamped-Clamped) (μm)	L	1000
Middle beam length (Cantilever) (μm)	L	503
Middle beam width (μm)	b	17.5
Grounded middle electrode width (μm)	b_1	30
Grounded side electrode width (μm)	b_2	288
Upper electrodes thickness (μm)	h	2
Lowwer electrodes thickness (μm)	h_1	0.5
Middle beam electrode gap (μm)	g_0	2
Side electrodes gap (μm)	g_1	2
Lateral distance (μm)	w	20.5
Elastic modulus (Gpa)	E	150
Density (kg/m^3)	ρ	2320
Poisson's ratio	ν	0.22
Air permitivity (pF/m)	ε_0	8.854
Characteristic height (μm)	$\bar{z}$	2

TABLE 2: Normalizing Parameters [19]

Parameter	Substitution
Nondimentonal length position	$x = \hat{x}/L$
Non-dimentional deflection	$w = \hat{w}/\bar{z}$
Non-dimentional time	$t = \hat{t}/T$
Non-dimentional damping	$\mathcal{C}^* = \alpha^2/\mathcal{Q}$
Area cross section(m^2)	$A = bh$
Moment of inertia(m^4)	$I = bh^3/12$
Time constant(s)	$T = \sqrt{\rho AL^4/EI}$
Mid-plane stretching constant	$r_1 = 6\left(\frac{g_0}{h}\right)^2$
Force constant(m/N)	$r_2 = L^4/EI\bar{z}$
1^{st} mode natural frequency	α
Quality factor	$\mathcal{Q}$

Adopting the framework of Euler-Bernoulli beam theory for an electro-mechanically coupled beam with out-of-plane (z) direction movement, neglecting the in-plane (y) deflection, because of the high width to thickness ratio, and including the stretching effect, the corresponding normalised governing equation for the out-of-plane motion of the repulsive force actuator, in non-dimensional form, can be written as [19]:

$$\frac{\partial^2 w}{\partial t^2} + \mathcal{C}^* \frac{\partial w}{\partial t} + \frac{\partial^4 w}{\partial x^4} - r_1 \left[\int_0^1 \left(\frac{\partial w}{\partial x} \right)^2 dx \right] \frac{\partial^2 w}{\partial x^2} + r_2 V^2 f_e(w) = 0, \tag{1}$$

where all the geometrical and normalizing parameters used in the above equation are listed in Tables 1 and 2. For the cantilever beam the stretching effect is negligible, i.e. we set $r_1 = 0$, while for the clamped-clamped beam, it is activated by setting $r_1 = 6$.

We perform a Galerkin-based reduced-order modelling (ROM) [4, 20, 21] on Equation (1) to approximate the moving electrode's resultant static/dynamic deflection (response) as follows:

$$w(x,t) = \sum_{i=1}^{N} U_i(t)\varphi_i(x), \tag{2}$$

The ROM process results in a system of coupled nonlinear ordinary differential equations in which U_i represents the generalized coordinates depending on time. The basis functions, $\varphi_i(x)$, have

TABLE 3: Mode shape natural frequencies and constants [19].

Mode	β_n^2(CL)	σ_n(CL)	β_n^2(CC)	σ_n(CC)
1	3.516	0.7341	22.3733	0.9825
2	22.035	1.01185	61.6728	1.00078
3	61.697	0.9992	120.903	0.9999

TABLE 4: Force constant defining for electrostatic force profile [3].

Symbol	Unit	value
$\mathcal{A}_0$	N/m	-1.1703×10^{-7}
$\mathcal{A}_1$	N/m^2	-3.8677×10^{-4}
$\mathcal{A}_2$	N/m^3	3.5574×10^{2}
$\mathcal{A}_3$	N/m^4	-1.2595×10^{7}
$\mathcal{A}_4$	N/m^5	1.7347×10^{11}
$\mathcal{A}_5$	N/m^5	-8.5695×10^{14}

the following form:

$$\varphi_i(x) = sin(\beta_n x) - sinh(\beta_n x) - \sigma_n \left[cos(\beta_n x) - cosh(\beta_n x) \right] \tag{3}$$

β_n denotes the square roots of the non-dimensionalized natural frequencies, and σ_n are constants determined from the boundary conditions and mode to be considered (see Table3). The most challenging step for the mathematical analysis of the system's behavior is to determine the equivalent value for the distributed electrostatic force and the generated levitation force per unit length ($f_e(w)$). For this, we adopt 2D finite element simulations, and we fit a polynomial function to the obtained electrostatic profile. This method has been experimentally validated [19]. A fit with a fifth-order polynomial accurately captured the profile, and the equivalent coefficients are listed in Table 4. The resulting system of ODEs can be written as [8]:

$$\sum_{i=1}^{N} \mathcal{M}_{ij}\ddot{U}_i(t) + \sum_{i=1}^{N} \mathcal{C}_{ij}\dot{U}_i(t) + \sum_{i=1}^{N} \mathcal{K}_{ij}U_i(t) - \sum_{i=1}^{N} \mathcal{S}_{ij}U_i^3(t) + F_j = 0 \tag{4}$$

where $\mathcal{M}$, $\mathcal{C}$, $\mathcal{K}$ and $\mathcal{S}$ are mass, damping, mechanical stiffness and stretching matrices, respectively, and F stands for the forcing vector. They are defined by:

$$\mathcal{M}_{ij} = \int_0^1 \varphi_i \varphi_j dx \qquad \mathcal{K}_{ij} = \int_0^1 \frac{d^2\varphi_i}{dx^2}\frac{d^2\varphi_j}{dx^2} dx$$

$$\mathcal{C}_{ij} = \mathcal{C}^*\mathcal{M}_{ij} \qquad \mathcal{S}_{ij} = r_1 \left[\int_0^1 \left(\frac{d\varphi_i}{dx} \right)^2 dx \right] \int_0^1 \varphi_j \frac{d^2\varphi_i}{dx^2} dx$$

$$F_j = r_2 V^2 \int_0^1 \sum_{k=0}^{5} \mathcal{A}_k \bar{x}^k \left(\sum_{i=1}^{N} U_i \varphi_i \right)^k \varphi_j dx \tag{5}$$

Modal interaction within a system requires that the ratio of the natural frequencies is close to rational. The natural frequencies are computed from the eigenvalues of the Jacobian matrix based on Equation (4) after excluding the damping term and evaluated at the fixed points (static equilibrium one) [22]. The experimental data for the first natural frequency of our system has been reported in [19]. To validate the numerical approach, we compare the corresponding results for the first natural frequency versus the applied DC voltage in Figure 3. We find that

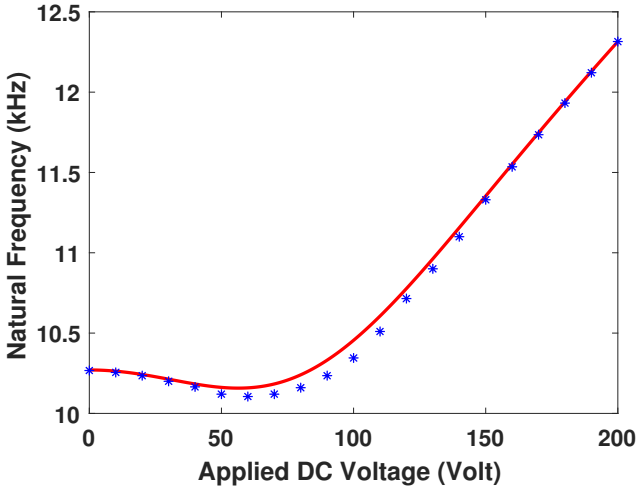

FIGURE 3: Comparison of the first natural frequency obtained from numerical (solid line) and experimental (dots) results [19].

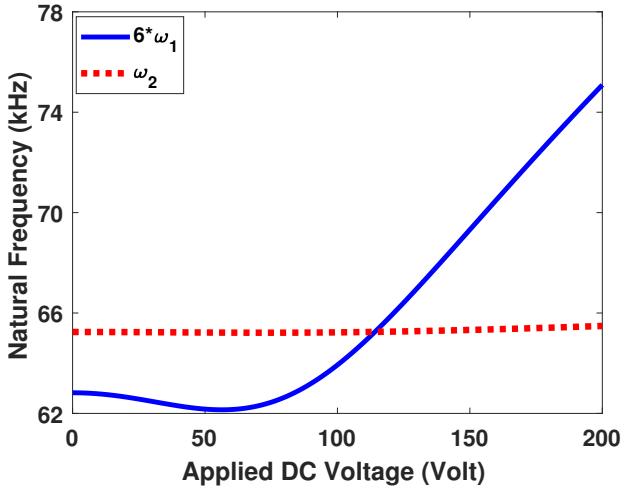

FIGURE 4: visual feasibility study chart in case of CL micro-beam with $L = 503$ micron for commensurate relation between first and second vibration modes.

we can reasonably predict the natural frequencies, although the slight difference comes from the effect of bottom dimples that are neglected in the numerical approach [19] . Furthermore, the numerical approach is capable of proper prediction for the falling-rising trend of the natural frequency which comes mainly from the hidden nature of the generated repulsive force in terms of applied DC voltage.

3. DYNAMIC RESPONSE EVALUATION USING MATCONT

In this section, we survey the numerical approaches for capturing the dynamic response of the repulsive electric micro-actuator. The objective is to obtain the frequency response as the beam is deflected by a DC load and vibrates by an AC harmonic load near its respective fundamental frequency. Typically, in any dynamical analysis, long-time integration for the ROM equations of motion can be used. However, this method suffers convergence problems near bifurcation points and, in general, is not considered a robust method for studying nonlinear vibrations. Other numerical approaches like the shooting method [23, 24] are highly sensitive to the initial conditions to find the periodic response. This problem exacerbates near bifurcations rendering the method ineffective. Because of the periodic forcing, the system exhibits a periodic response. This motivates to use the numerical continuation toolbox MatCont [25, 26]. It computes one-parameter families (branches) of periodic orbits of autonomous systems and obtain the Floquet multipliers to determine their stability as a function of the parameter, e.g., the forcing frequency. When the stability changes, we can easily find the corresponding bifurcation points. Freeing one more parameter, we can compute bifurcation curves in the parameter plane. MatCont works mainly using for autonomous first-order system [27]. So we reformulate the system of second-order ODEs (Eq.(5)) as a first-order system, and we use the Hopf normal form for the forcing, i.e., we augment the system with two ODEs

$$\begin{cases} X' = -\Omega Y + X(1 - X^2 - Y^2,) \\ Y' = \Omega X + Y(1 - X^2 - Y^2). \end{cases} \tag{6}$$

The variables X and Y evolve on the unit circle, and the term $cos(\Omega t)$ can be replaced with X. Next, we initialize the system with $X = 0$ and $Y = 1$ and $U_i = U_i' = 0$ and perform time integration for a sufficiently long time such transients have faded, and the state converged to the steady-state response. We then pick up the final point of this simulation and perform one more time integration for one forcing period. Through the "Select Cycle" feature, this last simulation is used as initial data for the numerical continuation, where we select the forcing frequency Ω and the period as free parameters. The continuation produces a sequence of points with an approximation of the periodic response for each parameter value. We plot the maximal amplitude of the variable U_1 as a function of the forcing frequency Ω. For terminology about bifurcations, we refer to [28].

4. RESULTS AND DISCUSSION

4.1 Exploration of internal resonance in case of CL

we assume that the numerical approach elaborated in the previous section is extendable for predicting the higher-order natural frequencies with similar accuracy. However, regarding the geometry of the moving element and the minimal effect of the asymmetric vibration m ode (third mode), governing equation of motion in this case is extended considering up to second vibration mode. Accordingly, Fig. 4 represents the prospect crossing of natural frequencies for micro cantilever beam with $L = 503$ microns, which might be considered the initial sign of six-to-one internal resonance between first and second frequencies. Generally, the figures indicate that for the applied DC voltage between 100 to 115 $Volt$, the system is susceptible to exhibit energy exchange but the previously detailed study in other MEMS system with the same moving unit [15], rules out the possibility of internal resonance due to the much lower amplitude of second mode compering to the corresponding one for the first mode. Consequently this case is deleted from our case studies as the possible internal resonance for cantilever micro-beam case as it demands a lower integer for the proportionality between first and second

vibration modes.

One useful and practical tool to confirm the previously reported results is Fast Fourier Transformation (FFT) which weights the modal contribution as presented in Figure 5 for each mode. Comparing the maximum of each mode, the contribution of the second mode is negligible to the first mode showing that energy exchange between the first and second mode is not feasible. Hence, in this case, it is justified to assume just one mode to predict the dynamic behavior of the system, which simplifies the governing equation of motion.

4.2 Exploration of internal resonance in case of CC

Following the similar approach as above (i.e. excluding the second mode considering the geometry of the system and modal interaction), we constructed the Jacobian matrix to calculate the natural frequencies up to third order, as shown in Fig. 6. Evaluating the results, we observe the potential case of 3:1 internal resonance between the first and third natural frequencies.

Fig. 6, visually stipulates that emerging the internal resonance in our system requires a range higher than the crossing threshold of $180V$ for applied DC voltage. We then vary the excitation frequency Ω to explore the frequency response of the system and possible energy exchange. Taking three vibrational modes and inserting the equation of motion into MatCont, Fig. 7 depicts the frequency response under applied DC voltage of 185 V.

To investigate the effect of increasing the applied DC and AC voltages on the nature and strength of internal resonance, we determined the frequency response for the first three modes (see Figure 9). Comparing the results depicted in Fig. 7 implies the expanding and intensifying effect of combined AC and DC voltage and upper starting point as the static equilibrium due to the applied DC voltage. Also, the sub-figures 9b, 9c , 9d show the detail of the response with the solid and dashed lines representing stable and unstable branches, respectively and marking the crucial points. Here LPC stands as saddle-node of periodic orbits while NS represents Neimark-Sacker of periodic orbits leading to a torus.

As the applied AC voltage can alter the result, the force response can be an instrumental diagram to explore the effect of increasing the applied AC voltage in a fixed applied DC voltage higher than the threshold coming from Fig. 6 and a fixed detuning frequency near emerging the internal resonance coming from 9. Figure 10 shows the effect on the response of the first and third mode of sweeping the applied AC voltage in four detuning excitation frequencies. The solid thick lines denote the Neimar-Sacker bifurcation ("Hopf for maps"), while solid and dotted lines depict the stable and unstable solution, respectively. The zoom-in Fig. 8 shows how an internal resonance develops near this voltage, and the third mode activates the energy exchange though with lower amplitude compared to the first vibration mode.

As principal parametric resonance was already reported experimentally [3] and validated mathematically [8], extending the frequency sweep in the vicinity of twice the primary resonance can be helpful. An important feature of MatCont is the detection of period-doubling (PD) bifurcation, where chaotic responses may arise. Continuing the forward sweep of the excitation frequency, we detected a PD point near $\Omega = 137.8$. The normal form coefficient computed by MatCont indicates this is a supercritical PD bifurcation, and this is shown in Figure 11. Here, the simulation near the detected PD point of the stable doubled response shows two dots in the Poincaré section. This diagram highlights the parametric internal resonance in our system, demanding more exhaustive and separated evaluation in this region.

5. CONCLUSION

This study evaluated the possibility of modal interaction in levitation force MEMS actuators. The overall outcomes of this investigation are summarized as follows: In the case of CL, the eigenvalue problem results predicts the occurrence of internal resonance between first and second vibration modes. Nevertheless, the commensurate relationship of this two modes was further examined using few dynamic simulations and FFT diagrams, and they both showed almost no possible modal interaction can occur among these two modes.

In the case of CC, the analysis implies that the first mode is proportional to the third mode with a factor of 3. This possibility of internal resonance was examined again using frequency responses curves which all showed the two modes interaction with softening-hardening trends very useful for sensing applications.

The effect of increasing the AC voltage increasing the a fixed DC voltage was assessed with excitation frequencies varying in the neighborhood of the internal resonance area. The generated frequency responses showed few the cyclic fold and Hopf bifurcations via constructed Jacobian matrix. Finally, examining the frequency response in the vicinity of twice the primary resonance led to the detection of a period-doubling point supporting the potential of parametric internal resonance for the examined system. Phase plots and Poincaré section diagrams were also generated for further evaluation in the vicinity of the internal resonance occurrence area. Such diagrams were also useful in detecting some hidden characteristics and new features of the structure and provided further evidences of the occurrence of possible chaotic behavior of the system within this internal resonance region. The general assessment of this work stipulates that the geometry and dimension of the moving part (the microbeam) are dominant factors in creating modal interaction that can be further studied to design smart mass sensors based on modal-interaction.

REFERENCES

[1] Zamanzadeh, M, Pournaki, I Jafarsadeghi and Azizi, S. "Bifurcation Analysis of the Levitation Force MEMS Actuators." *International Journal of Mechanical Sciences* (2020): p. 105614.

[2] Zamanzadeh, Mohammadreza and Azizi, Saber. "Static and dynamic characterization of micro-electro-mechanical system repulsive force actuators." *Journal of Vibration and Control* (2019): p. 1077546319892131.

[3] Pallay, Mark and Towfighian, Shahrzad. "A parametric electrostatic resonator using repulsive force." *Sensors and Actuators A: Physical* Vol. 277 (2018): pp. 134–141.

[4] Zamanzadeh, Mohammadreza, Rezazadeh, Ghader, Jafarsadeghi-Poornaki, Ilgar and Shabani, Rasool. "Static

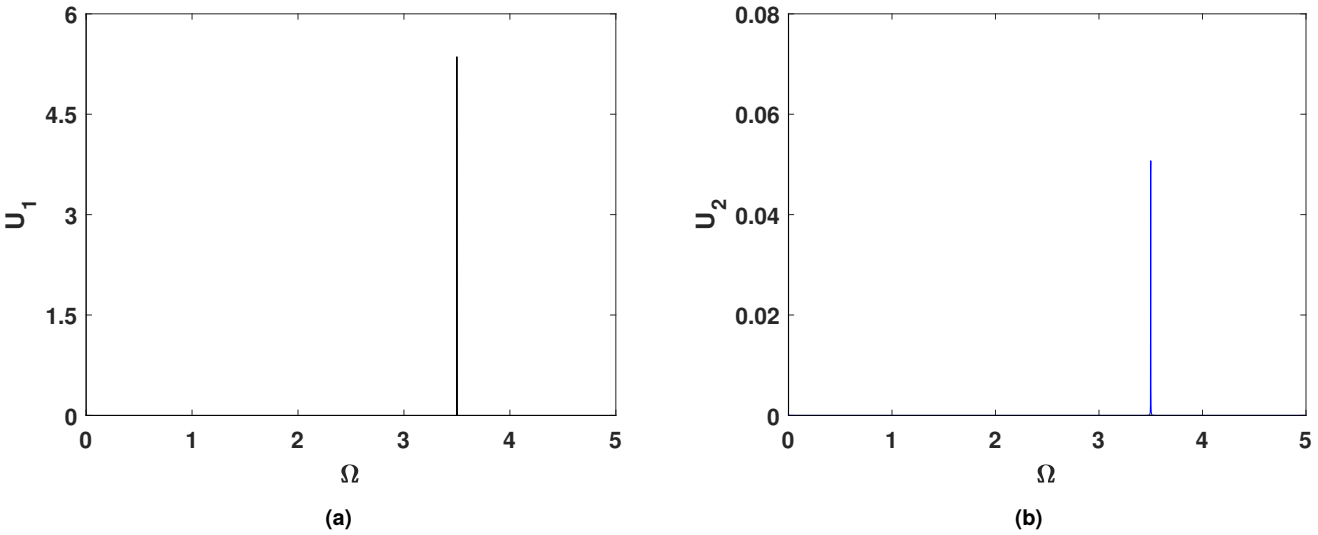

FIGURE 5: FFT in case of CL micro beam at $V_{DC} = 130V, V_{AC} = 1.5V$.

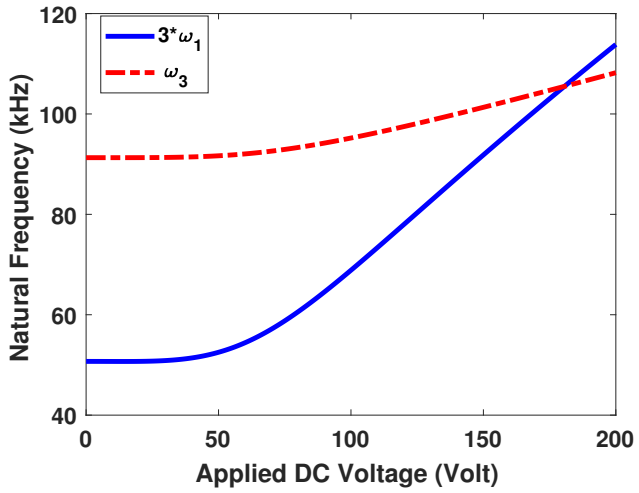

FIGURE 6: Crossing feasibility and corresponding integer between proportional natural frequencies in CC micro-beam.

and dynamic stability modeling of a capacitive FGM micro-beam in presence of temperature changes." *Applied Mathematical Modelling* Vol. 37 No. 10-11 (2013): pp. 6964–6978.

[5] Jafarsadeghi-pournaki, Ilgar, Rezazadeh, Ghader, Zamanzadeh, Mohammadreza and Shabani, Rasool. "Thermally induced vibration of an electro-statically deflected functionally graded micro-beam considering thermo-elastic coupling effect." *Scientia Iranica* Vol. 21 No. 3 (2014): pp. 647–662.

[6] Madinei, Hadi, Zamanzadeh, Mohammad, Jafarsadeghi-pournaki, Ilgar and Rezazadeh, Ghader. "Static pull-in analysis of capacitive FGM nanocantilevers subjected to thermal moment using Eringen's nonlocal elasticity." *International Journal of Engineering* Vol. 27 No. 4 (2014): pp. 633–642.

[7] Jafarsadeghi-Pournaki, Ilgar, Rezazadeh, Ghader, Zamanzadeh, Mohammadreza and Shabani, Rasoul. "Parametric thermally induced vibration of an electrostatically deflected FGM micro-beam." *International Journal of Applied Mechanics* Vol. 8 No. 08 (2016): p. 1650092.

[8] Zamanzadeh, Mohammadreza, Ouakad, Hassen M and Azizi, Saber. "Theoretical and experimental investigations of the primary and parametric resonances in repulsive force based MEMS actuators." *Sensors and Actuators A: Physical* Vol. 303 (2020): p. 111635.

[9] Pallay, Mark, Miles, Ronald N and Towfighian, Shahrzad. "Merging parallel-plate and levitation actuators to enable linearity and tunability in electrostatic MEMS." *Journal of Applied Physics* Vol. 126 No. 1 (2019): p. 014501.

[10] Zamanzadeh, Mohammadreza, Jafarsadeghi-Pournaki, Ilgar and Ouakad, Hassen M. "A resonant pressure MEMS sensor based on levitation force excitation detection." *Nonlinear Dynamics* .

[11] Pallay, Mark, Miles, Ronald N and Towfighian, Shahrzad. "A tunable Electrostatic MEMS Pressure Switch." *IEEE Transactions on Industrial Electronics* .

[12] Westra, HJR, Karabacak, DM, Brongersma, SH, Crego-Calama, M, Van Der Zant, HSJ and Venstra, WJ. "Interactions between directly-and parametrically-driven vibration modes in a micromechanical resonator." *Physical Review B* Vol. 84 No. 13 (2011): p. 134305.

[13] Asadi, Keivan, Yu, Jun and Cho, Hanna. "Nonlinear couplings and energy transfers in micro-and nano-mechanical resonators: intermodal coupling, internal resonance and synchronization." *Philosophical Transactions of the Royal Society A: Mathematical, Physical and Engineering Sciences* Vol. 376 No. 2127 (2018): p. 20170141.

[14] Younis, Mohammad Ibrahim and Nayfeh, AH. "A study of the nonlinear response of a resonant microbeam to an electric actuation." *Nonlinear Dynamics* Vol. 31 No. 1 (2003): pp. 91–117.

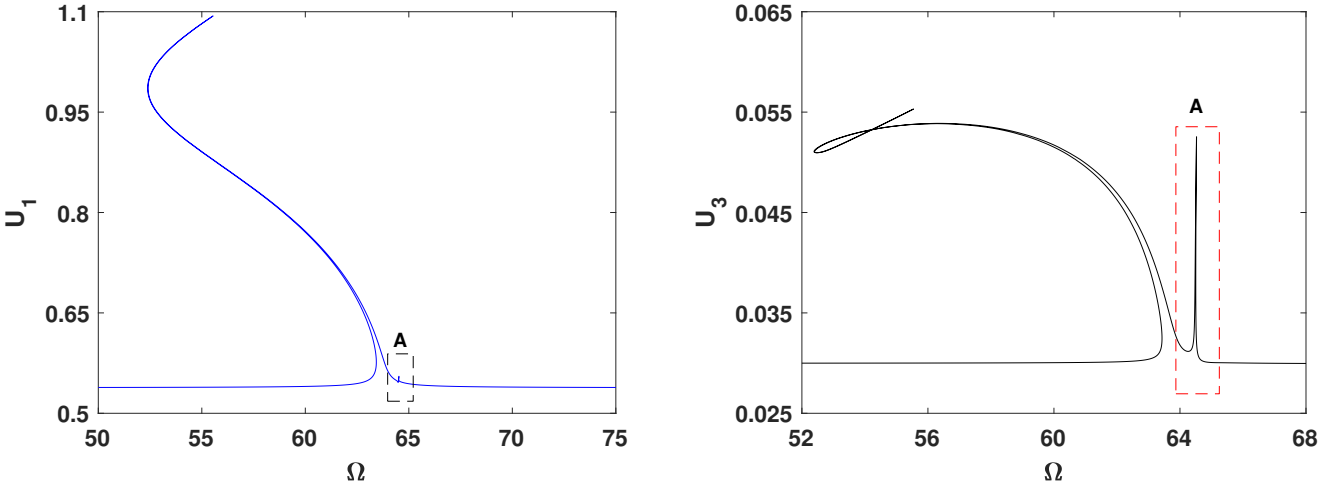

(a) first vibration mode

(b) third vibration mode

FIGURE 7: Frequency response of the second vibration mode at $V_{DC} = 185V$ and $V_{AC} = 0.1V$.

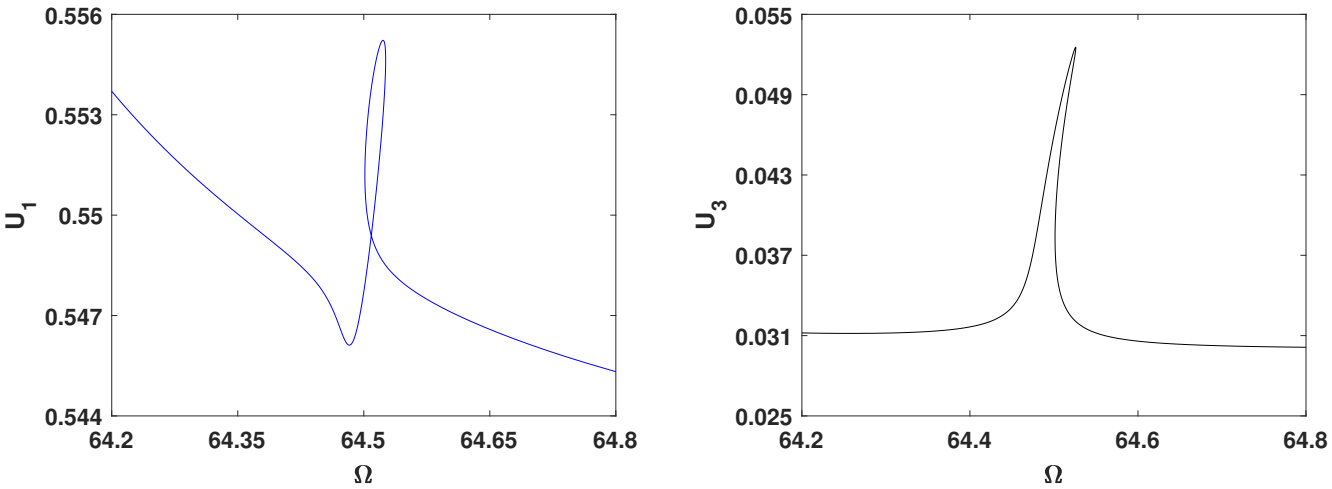

(a) first vibration mode

(b) third vibration mode

FIGURE 8: Frequency response of the zoom-in region for Fig. 7.

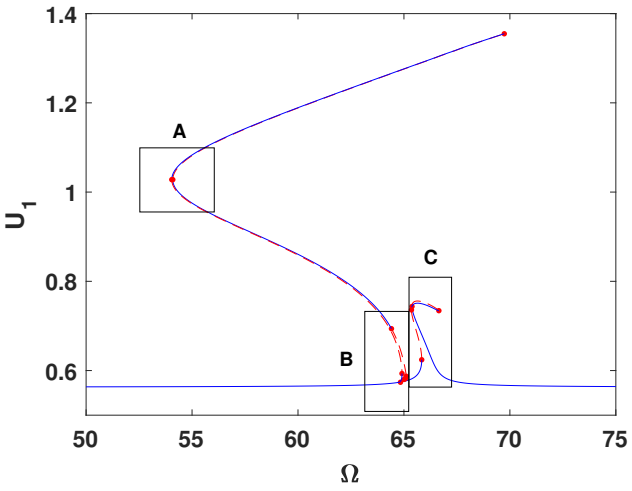

(a) first vibration mode

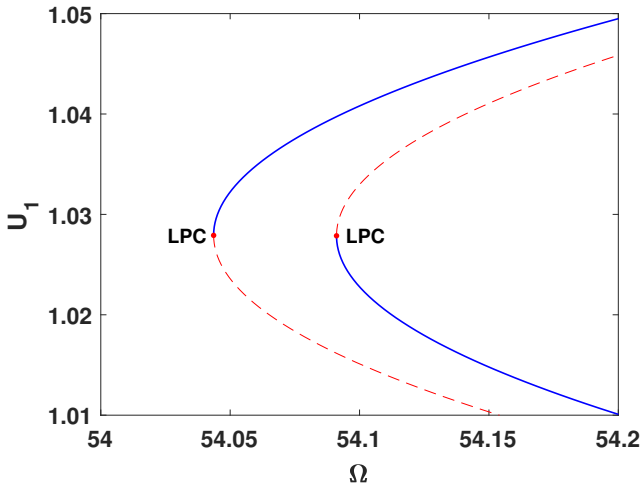

(b) zoom-in region A

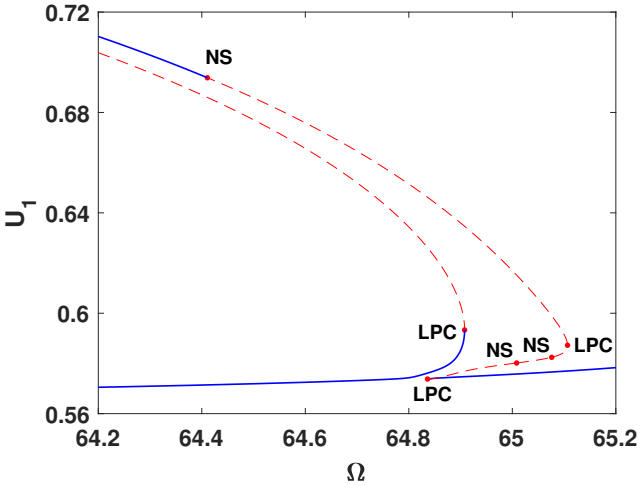

(c) zoom-in region B

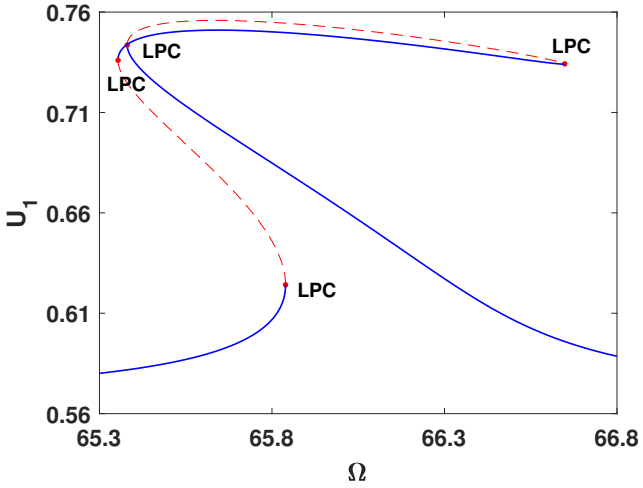

(d) zoom-in region C

FIGURE 9: Frequency response of the first vibration mode at $V_{DC} = 195V$ and $V_{AC} = 0.2V$.

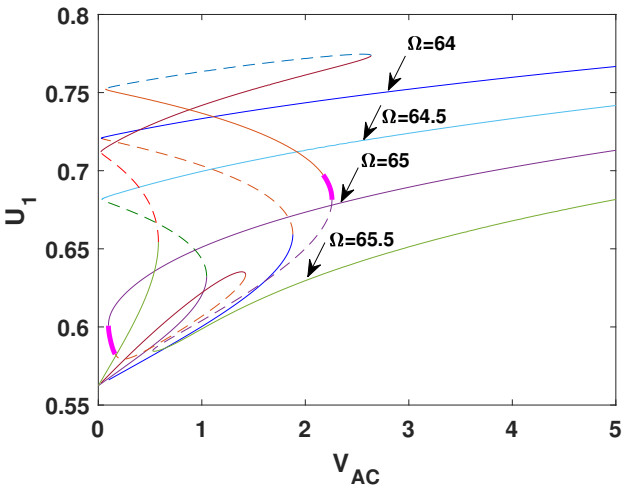

(a) first vibration mode

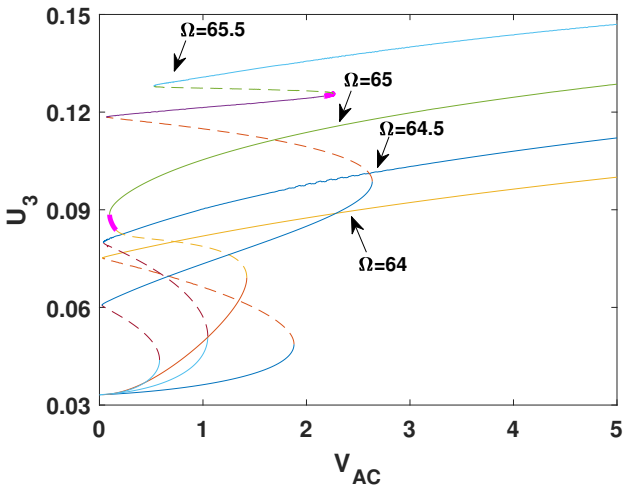

(b) third vibration mode

FIGURE 10: Force response at $V_{DC} = 195V$.

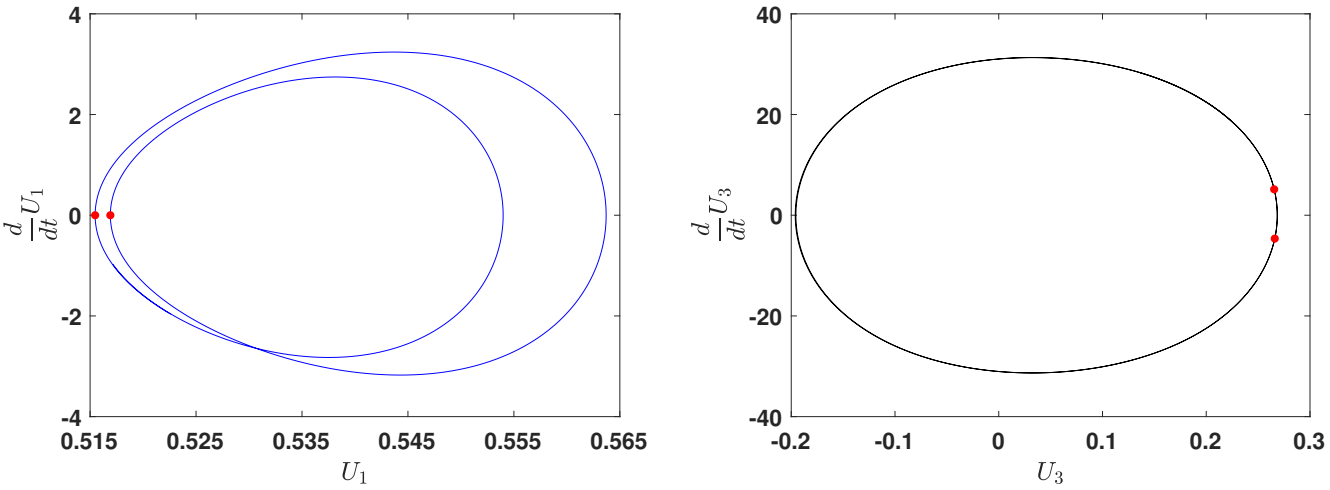

(a) first vibration mode **(b) third vibration mode**

FIGURE 11: Phase plane and Poincaré section at PD points detected by MatCont with Ω = 137.8.

[15] Ghayesh, Mergen H and Farokhi, Hamed. "Size-dependent internal resonances and modal interactions in nonlinear dynamics of microcantilevers." *International Journal of Mechanics and Materials in Design* Vol. 14 No. 1 (2018): pp. 127–140.

[16] Kumar, Praveen, Inamdar, Mandar M and Pawaskar, Dnyanesh N. "Characterisation of the internal resonances of a clamped-clamped beam MEMS resonator." *Microsystem Technologies* (2020): pp. 1–17.

[17] Ouakad, Hassen M, Sedighi, Hamid M and Younis, Mohammad I. "One-to-one and three-to-one internal resonances in MEMS shallow arches." *Journal of Computational and Nonlinear Dynamics* Vol. 12 No. 5.

[18] Wang, Ze and Ren, Jianting. "Three-to-One Internal Resonance in MEMS Arch Resonators." *Sensors* Vol. 19 No. 8 (2019): p. 1888.

[19] Pallay, Mark, Daeichin, Meysam and Towfighian, Shahrzad. "Dynamic behavior of an electrostatic MEMS resonator with repulsive actuation." *Nonlinear Dynamics* Vol. 89 No. 2 (2017): pp. 1525–1538.

[20] Younis, Mohammad I, Abdel-Rahman, Eihab M and Nayfeh, Ali. "A reduced-order model for electrically actuated microbeam-based MEMS." *Journal of Microelectromechanical systems* Vol. 12 No. 5 (2003): pp. 672–680.

[21] Ouakad, Hassen M. "Electrostatic fringing-fields effects on the structural behavior of MEMS shallow arches." *Microsystem Technologies* Vol. 24 No. 3 (2018): pp. 1391–1399.

[22] Younis, Mohammad I. *MEMS linear and nonlinear statics and dynamics*. Vol. 20. Springer Science & Business Media (2011).

[23] Ouakad, Hassen M, Najar, Fehmi and Hattab, Oussama. "Nonlinear analysis of electrically actuated carbon nanotube resonator using a novel discretization technique." *Mathematical Problems in Engineering* Vol. 2013.

[24] Ouakad, Hassen M and Younis, Mohammad I. "Nonlinear dynamics of electrically actuated carbon nanotube resonators." *Journal of computational and nonlinear dynamics* Vol. 5 No. 1.

[25] Dhooge, A, Govaerts, W, Kuznetsov, Yu A, Mestrom, W, Riet, AM and Sautois, B. "MATCONT and CL MATCONT: Continuation toolboxes in matlab." *Universiteit Gent, Belgium and Utrecht University, The Netherlands* .

[26] Meijer, Hil. "Matcont tutorial: ODE GUI version." (2016).

[27] Dhooge, Annick, Govaerts, Willy and Kuznetsov, Yu A. "MATCONT: a Matlab package for numerical bifurcation analysis of ODEs." *ACM SIGSAM Bulletin* Vol. 38 No. 1 (2004): pp. 21–22.

[28] Kuznetsov, Yuri A. "Topological equivalence, bifurcations, and structural stability of dynamical systems." *Elements of Applied Bifurcation Theory*. Springer (2004): pp. 39–76.